

This article was downloaded by:

On: 26 January 2011

Access details: *Access Details: Free Access*

Publisher *Taylor & Francis*

Informa Ltd Registered in England and Wales Registered Number: 1072954 Registered office: Mortimer House, 37-41 Mortimer Street, London W1T 3JH, UK



## Liquid Crystals

Publication details, including instructions for authors and subscription information:

<http://www.informaworld.com/smpp/title~content=t713926090>

### Phases and phase transitions in a nematic lyotropic system with a biaxial phase

F. P. Nicolettat<sup>a</sup>; G. Chidichimo<sup>b</sup>; A. Golemme<sup>b</sup>; N. Picci<sup>b</sup>

<sup>a</sup> Dipartimento di Fisica, GNSM and INFM Unità di Cosenza, Università della Calabria, Arcavacata di Rende (Cosenza), Italy <sup>b</sup> Dipartimento di Chimica, Università della Calabria, Arcavacata di Rende (Cosenza), Italy

**To cite this Article** Nicolettat, F. P. , Chidichimo, G. , Golemme, A. and Picci, N.(1991) 'Phases and phase transitions in a nematic lyotropic system with a biaxial phase', *Liquid Crystals*, 10: 5, 665 – 674

**To link to this Article:** DOI: 10.1080/02678299108241734

**URL:** <http://dx.doi.org/10.1080/02678299108241734>

PLEASE SCROLL DOWN FOR ARTICLE

Full terms and conditions of use: <http://www.informaworld.com/terms-and-conditions-of-access.pdf>

This article may be used for research, teaching and private study purposes. Any substantial or systematic reproduction, re-distribution, re-selling, loan or sub-licensing, systematic supply or distribution in any form to anyone is expressly forbidden.

The publisher does not give any warranty express or implied or make any representation that the contents will be complete or accurate or up to date. The accuracy of any instructions, formulae and drug doses should be independently verified with primary sources. The publisher shall not be liable for any loss, actions, claims, proceedings, demand or costs or damages whatsoever or howsoever caused arising directly or indirectly in connection with or arising out of the use of this material.

## Phases and phase transitions in a nematic lyotropic system with a biaxial phase

by F. P. NICOLETTA<sup>†</sup>, G. CHIDICHIMO<sup>†\*</sup>,  
A. GOLEMME<sup>‡</sup> and N. PICCI<sup>‡</sup>

Dipartimento di Fisica, GNSM and INFN Unità di Cosenza<sup>†</sup>, Dipartimento di Chimica<sup>‡</sup>, Università della Calabria, 87036 Arcavacata di Rende (Cosenza), Italy

(Received 26 November 1990; accepted 26 May 1991)

NMR spectroscopy and optical microscopy have been used to study phase transitions and structure in nematic lyotropic mesophases formed by potassium laurate, decylammonium hydrochloride and water. The different mesophases obtained in a well-defined composition range have been characterized, by deuterium NMR, following the evolution of the  $D_2O$  spectra as a function of temperature and of the orientation of the samples with respect to the magnetic field. Wide ranges of biaxiality have been found and the asymmetry parameter of the averaged electrical field gradient tensor on the deuterium of the  $D_2O$  molecule has been determined. The presence of the different mesophases has always been confirmed by observing oriented samples under the polarizing optical microscope.

### 1. Introduction

Mixtures of amphiphilic molecules and water may form nematic lyotropic liquid crystals characterized by aggregates of amphiphiles with definite shape. Although other terminology has been employed, the resulting phases are often referred to, by considering their magnetic and optical properties, as positive uniaxial, biaxial and negative uniaxial nematics [1-3]. Such systems occur in a concentration range between the isotropic micellar phase, formed by small spherical aggregates, and the hexagonal, or lamellar, phases, in which the aggregates are infinite cylinders with bidimensional hexagonal symmetry or infinite lamellae in a unidimensional lattice [4]. The micellar shape in the three lyotropic nematic mesophases still constitutes one unsettled subject. According to early studies there are three different shapes: discotic,  $N_D$ , cylindrical,  $N_C$ , and 'biaxial',  $N_{bx}$  [1, 2]. The micelles change their shape continuously from disc-like to cylinder-like passing through a biaxial shaped aggregate. Recently, X-ray diffraction measurements have suggested that the intrinsic micellar shape is always biaxial and the different nematic mesophases are the result of overall fluctuations [3].

We have studied the potassium laurate/decylammonium hydrochloride/heavy water system by deuterium NMR and optical microscopy. The choice of this particular system has been suggested by a recent work [5] in which the potassium laurate/decylammonium hydrochloride/light water has been shown to exhibit all three nematic phases and to be more stable in time with respect to the analogous systems containing alcohols [1, 2] because esterification does not occur. In this work we intend to show how extremely simple and fast deuterium NMR measurements can be used to determine the phase boundaries of the samples and the sign of the anisotropy of

\* Author for correspondence.

diamagnetic susceptibility,  $\Delta\chi$ . The polarization microscope in orthoscopic and conosopic observation was used to distinguish among the different nematic phases and to determine the sign of the birefringence.

## 2. Experimental methods

Potassium laurate (KL) was prepared under nitrogen by dissolving lauric acid (from Aldrich, recrystallized from methanol/water, vacuum dried and with  $mp = 45^\circ\text{C}$ ) in dry methanol and neutralizing with a dry potassium hydroxide 0.1 N methanolic solution. KL, before use, was twice recrystallized from dry methanol. Decylammonium hydrochloride (DaCl) was prepared under nitrogen by addition of gaseous hydrochloric acid to an anhydrous diethyl ether solution of decylamine (from Aldrich, twice vacuum distilled and with  $bp = 100^\circ\text{C}/11\text{ mm Hg}$ ). DaCl, before use, was twice recrystallized from dry ethanol/petroleum ether 1:4 *v/v* [6].

Samples were prepared by weighing the appropriate amounts of the compounds, with 0.05 mg accuracy, in glass tubes. The mixtures were shaken and centrifuged until they were homogeneous between crossed polarizers. They were then flame sealed to avoid water loss.

### 2.1. Optical microscopy and conosopic measurements

The samples were sealed in flat microslides (from Vitrodynamics, U.S.A.), 200  $\mu\text{m}$  wide and placed on a hot stage (Linkam TH600) with a  $0.1^\circ\text{C}$  accuracy. Optical microscopy was performed on a C. Zeiss Axioplan microscope equipped for orthoscopic and conosopic observation. After capillary filling, the disc-like nematic phase is not oriented but the polar interactions between the glass surface and the micelles orient them in a homeotropic texture, in which the optical axes are parallel to the short microslide axis, i.e. the 200  $\mu\text{m}$  axis which is also the observation axis. Cylinder-like nematics prefer to remain with their optical axes parallel to the surface [1]. In order to homogenize the spontaneous alignment of the disc phase we inserted the microslides in a magnetic field before microscope observations.

### 2.2. Deuterium NMR spectroscopy

The quadrupolar spectra from  $\text{D}_2\text{O}$  were recorded on a Varian XL100 spectrometer with a temperature control accuracy of  $\pm 0.5^\circ\text{C}$  and a magnetic field of  $\sim 23\text{ kG}$ . Mesophases were characterized by following the evolution of the  $\text{D}_2\text{O}$  spectra as a function of temperature and of sample orientation with respect to the magnetic field. In particular we have performed for each temperature three different NMR measurements:

- (1) static measurements;
- (2) measurements after a  $\pi/2$  rotation of the sample about an axis normal to the external field;
- (3) measurements with the sample spinning about an axis normal to the external field.

We must recall that the  $\pi/2$  rotation measurement was performed immediately after the sample rotation and that the spinning rate was  $\sim 2\text{ Hz}$ , in order to avoid inertial effects [7] and to obtain reproducible spectra. In the following we will see the utility of such experiments for our purpose.

The reduced quadrupolar resonance for  $D_2O$  in a nematic liquid crystal is given by [8]

$$v_{\pm} = \pm \frac{3}{4} \bar{v} \left[ \frac{3 \cos^2 \theta_0 - 1}{2} + \frac{\eta \sin^2 \theta_0 \cos 2\phi_0}{2} \right], \quad (1)$$

where  $\bar{v}$  is the partially averaged quadrupolar coupling constant,  $\theta_0$  and  $\phi_0$  are the polar and azimuthal angles of the external magnetic field in the phase reference frame, i.e. the phase symmetry axes,  $\eta$  is the asymmetry parameter. This is zero for the  $N_D$  and  $N_C$  phases, and is given by  $(V_{xx} - V_{yy})/V_{zz}$ , as a function of the field gradient tensor components, according to the usual convention  $|V_{xx}| < |V_{yy}| < |V_{zz}|$ , i.e. the reference frame has to have the  $z$  axis along the largest component of the electrical field gradient tensor.

Lytropic nematic phases are usually oriented by magnetic fields of the intensity of the ones used for NMR experiments (several Teslas). This means that the angle  $\theta_0$  (and  $\phi_0$  in the case of  $\eta \neq 0$ ) is well defined and it is the same over all the sample. In this case the spectral lineshape consists of two peaks separated by  $\Delta v = v_+ - v_-$ .

It is clear from equation (1) that the quadrupolar splitting is sensitive to the external field orientation with respect to the diamagnetic susceptibility tensor symmetry axes. This property can be used, among other things, to determine the sign of the anisotropy of the diamagnetic susceptibility of a lyotropic phase. As an example let us consider a uniaxial phase, like the  $N_D$  or the  $N_C$ , i.e. a phase for which  $\eta = 0$ . When we take a spectrum from such a sample we obtain two lines separated by  $\Delta v$ . We can then take another spectrum immediately after a  $\pi/2$  rotation about an axis normal to the external field. If the sample reorientation under the effect of the magnetic field is slow compared to the measurement time, then we will see a different spectrum. For a sample with  $\Delta\chi > 0$ , for example, we will see a doublet with separation  $\Delta v/2$ , corresponding to a change from  $\theta_0 = 0$  to  $\theta_0 = \pi/2$  in equation (1). (The sign of the diamagnetic anisotropy is referred to the symmetry axis of the phase.)

Information about the phase orientation and parameters can also be obtained by spinning experiments. The angles  $\theta_0$  and  $\phi_0$  of equation (1) may change orientation as a result of the spinning. If they do then the total quadrupolar splitting will change. Two regimes can be separated in this case. If the spinning rate is much larger than  $\bar{v}$  the effect of spinning is a further averaging of  $\bar{v}$  and the resulting splitting will be a doublet. If instead the spinning rate is much smaller than  $\bar{v}$ , the angles that change orientation will contribute to the spectrum with all their possible values. This case can help us not only to determine the sign of  $\Delta\chi$  but also to measure  $\bar{v}$  and  $\eta$  in the biaxial phases. In all our experiments we have used a spinning rate of  $\sim 2$  Hz, i.e. we were in this slow spinning regime.

### 3. Results and discussion

Figure 1 shows the phase diagram of the mixture KL/DaCl/ $D_2O$  at fixed amphiphil/water molar ratio

$$\frac{[\text{KL}] + [\text{DaCl}]}{[\text{D}_2\text{O}]} = 0.05$$

obtained by varying the relative molar ratio of the two amphiphiles

$$R = \frac{[\text{DaCl}]}{[\text{KL}]} \quad 0.13 < R < 0.17.$$

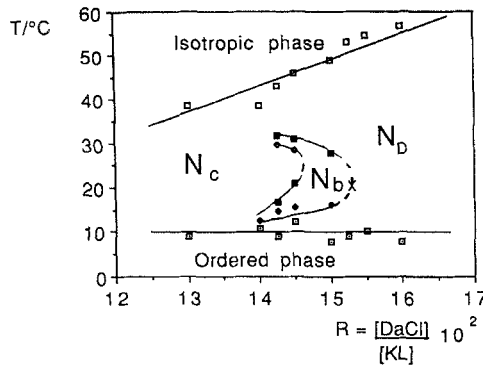


Figure 1. The phase diagram for the KL/DaCl/D<sub>2</sub>O system (I, isotropic; N<sub>D</sub>, discotic nematic; N<sub>bx</sub>, biaxial nematic; N<sub>C</sub>, cylindric nematic). This phase diagram is obtained at constant amphiphile/water molar ratio, 0.05, and 0.13 < *R* < 0.17. *R* is the relative molar ratio of the two amphiphiles.

The phase diagram was obtained by following the temperature evolution of the quadrupole splittings observed for static, after a  $\pi/2$  sample rotation and spinning samples. Each nematic mesophase can be characterized by a well-defined set of lineshapes, as a function of the kind of the performed measurement, as we will show in detail later. The phase diagram of figure 1 is quite different in shape from the analogous diagram, obtained in samples with light water reported in [4] and there is no inversion of the uniaxial mesophases position with temperature. Our phase diagram is instead very similar to that reported by Yu and Saupe in the KL/decanol/D<sub>2</sub>O mixture [1].

The existence of the three nematic mesophase was always confirmed by optical microscopy and conoscopic observations of the same samples in flat capillaries. Homogeneous textures appeared in the discotic nematic phase and random orientational defects in the biaxial nematic phase. For the determination of the optical character of the nematic mesophases we performed conoscopic observation of our samples. Lyotropic nematics have one or two optical axes and a positive or negative character. A uniaxial mesophase, aligned in such a way that the optical axis is parallel to the direction of observation, shows a dark cross (surrounded by interference fringes) in conoscopic observation. By inserting a lambda plate, the white north-east quadrant, determined by this cross, will change to yellow if the mesophase is optically negative and to blue if it is optically positive. The conoscopic interference pattern of a biaxial liquid crystal consists of two hyperbola legs which determine three sides: an inner or convex side and two outer or concave sides. When these legs are in the first and third quadrant the insertion of the lambda plate will turn the white inner side to blue and the white outer sides to yellow if the liquid crystal is optically negative, the opposite, i.e. to yellow and to blue respectively, if the mesophase is optically positive [9]. In such a way we derived that the N<sub>D</sub> phase has a negative birefringence, the N<sub>C</sub> phase has a positive birefringence and the N<sub>bx</sub> changes its optical sign with temperature.

Detailed information about the phase diagram and biaxiality can be deduced from NMR spectra obtained for the different nematic mesophases [10]. Typical spectral lineshapes are reported in figure 2. Let us consider first the two phases that were identified as uniaxial N<sub>D</sub> and N<sub>C</sub> phases under the optical microscope. In the N<sub>D</sub> phase the spectrum obtained after a  $\pi/2$  rotation is a typical 'cylindrical' spectrum, i.e. it derives from the distribution of  $\theta_0$  around  $\mathbf{H}_0$  with every  $0 < \theta_0 < \pi$  equally probable.

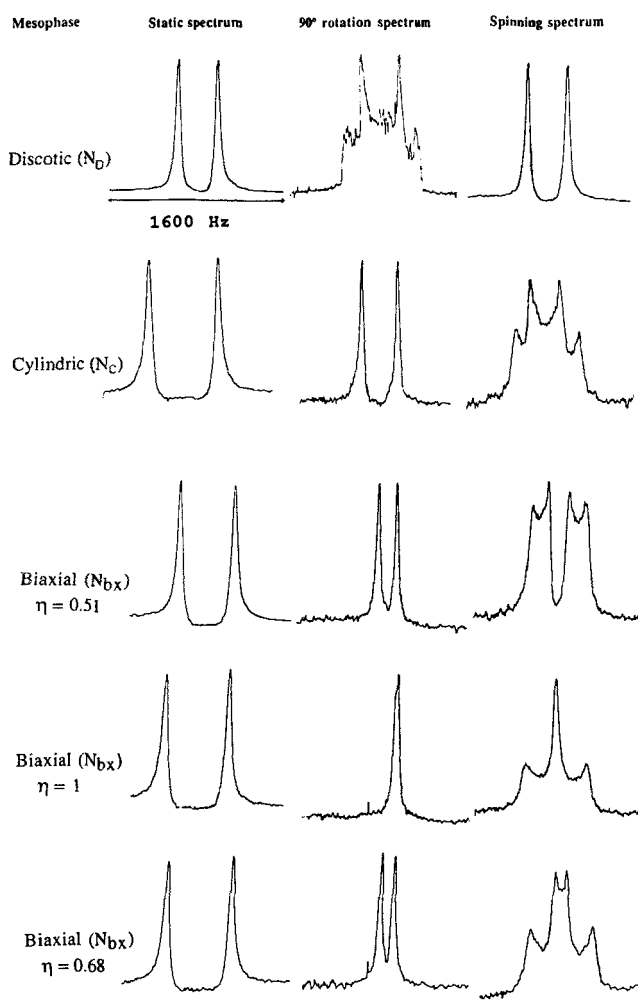


Figure 2. Typical deuterium NMR spectra of  $D_2O$  observed in the three nematic phases of the sample with  $R = 0.1450$  during the three different measurements: static, after  $\pi/2$  rotation and spinning. The difference in the biaxial spectra arise both from the different value of  $\eta$  and from the fact that the phase symmetry axes are oriented as in figure 3(a) for the first two cases and as in figure 3(b) for the last case.

To explain such behaviour we need to consider that during the measurement time, that is the time necessary to acquire a single scan spectrum, in our case always less than 100ms, the orientation of our samples does not change substantially. In fact, a disordered sample is aligned by our magnetic field only after a few minutes and the spectrum recorded after the  $\pi/2$  rotation is obtained within 3 s from the rotation itself, using only one scan. The spinning spectra are instead identical to the static one. They are obtained by accumulating scans and thus they reflect the distribution of  $\theta_0$  and  $\phi_0$  due to the rotation. The spectra obtained for the  $N_D$  phase are then easily understood if we consider the static spectrum as derived from a director orientation perpendicular to the magnetic field ( $\theta_0 = \pi/2$ ) but with all the possible orientations within the plane normal to  $\mathbf{H}_0$ . After the  $\pi/2$  rotation such orientations correspond to different  $\theta_0$ s and

Table 1. Values of the angles  $\theta_0$  and  $\phi_0$  for different phases. The two different biaxial cases,  $N_{\text{bxa}}$  and  $N_{\text{bxb}}$ , are the two cases shown in figure 3.

Mesophase	Static	$\pi/2$ rotation	Spinning
$N_D$	$\theta_0 = \frac{\pi}{2}, \eta = 0$	$\theta_0 = \text{distr.}, \eta = 0$	$\theta_0 = \frac{\pi}{2}, \eta = 0$
$N_{\text{bxa}}$	$\theta_0 = \frac{\pi}{2}, \phi_0 = \frac{\pi}{2}$	$\theta_0 = \frac{\pi}{2}, \phi_0 = 0$	$\theta_0 = \frac{\pi}{2}, \phi_0 = \text{distr.}$
$N_{\text{bxb}}$	$\theta_0 = 0$	$\theta_0 = \frac{\pi}{2}, \phi_0 = 0$	$\theta_0 = \text{distr.}, \phi_0 = 0$
$N_C$	$\theta_0 = 0, \eta = 0$	$\theta_0 = \frac{\pi}{2}, \eta = 0$	$\theta_0 = \text{distr.}, \eta = 0$

Table 2. Values of quadrupolar splittings of  $D_2O$  molecules in the different phases.  $N_{\text{bxa}}$  and  $N_{\text{bxb}}$  refer to the two cases shown in figure 3. In the cases when the spectrum is not a single doublet the angle dependent reduced resonance frequency is given.

Mesophase	Static	$\pi/2$ rotation	Spinning
$N_D$	$\frac{3}{4}\bar{\nu}$	$\frac{3}{4}\bar{\nu}[3\cos^2\theta_0 - 1]$	$\frac{3}{4}\bar{\nu}$
$N_{\text{bxa}}$	$\frac{3}{4}\bar{\nu}[1 + \eta]$	$\frac{3}{4}\bar{\nu}[1 - \eta]$	$\frac{3}{4}\bar{\nu}[-1 + \eta\cos 2\phi_0]$
$N_{\text{bxb}}$	$\frac{3}{2}\bar{\nu}$	$\frac{3}{4}\bar{\nu}[1 - \eta]$	$\frac{3}{4}\bar{\nu}[3\cos^2\theta_0 - 1 + \eta\sin^2\theta_0]$
$N_C$	$\frac{3}{2}\bar{\nu}$	$\frac{3}{4}\bar{\nu}$	$\frac{3}{4}\bar{\nu}[3\cos^2\theta_0 - 1]$

this is why we obtain the spectrum shown in figure 2. The spinning of the sample, instead, forces the director to orient along the only direction normal to  $\mathbf{H}_0$  which is not disturbed by sample rotation, i.e. the axis around which the sample spins. In this case when the spectrum obtained is identical to the static one, even if the distribution of the director orientation is quite different. It is important to underline that the spinning spectra are recorded only after 10 min of sample spinning, to let the director orientation reach equilibrium under such conditions. A summary of the director orientation and the resulting main spectral features for the different phases and experimental conditions is listed in tables 1 and 2, respectively.

Let us consider now the spectra obtained for the  $N_C$  phase and shown in figure 2. First of all we notice that the static spectrum has a splitting about twice as large as the corresponding spectrum from the  $N_D$  phase. This indicates that the director is, in this case, oriented along the magnetic field. This is confirmed by the fact that the spectrum taken after the  $\pi/2$  rotation is exactly half as wide, i.e. from  $\theta_0 = 0$  we obtain  $\theta_0 = \pi/2$  over the whole sample. By spinning the sample,  $\theta_0$  is distributed over a plane containing  $\mathbf{H}_0$  and again a spectrum corresponding to a cylindrical pattern is obtained. In this spectrum two sets of singularities are observed, the external ones corresponding to the singularities of the static spectrum and the internal ones to the singularities of the  $\pi/2$  rotated spectrum.

The interpretation of the biaxial spectra in figure 2 is not as simple as in the case of those obtained for the  $N_D$  and  $N_C$  phases. The first feature of these spectra to be underlined is that both the static spectrum and that obtained after the  $\pi/2$  rotation are doublets, i.e. in this case there are only two frequencies of resonance. This means that, since  $\eta \neq 0$ , the angles  $\theta_0$  and  $\phi_0$  of equation (1) must have a well-defined value, which is the same over the whole sample. A second feature of these spectra is that there are two possible orientations of the magnetic field with respect to the phase symmetry axes which are in agreement with the observed spectra. To better understand the origin of the observed orientation of the phase symmetry axes with respect to the magnetic field, it is necessary to consider our experimental procedure. All of our spectra have been taken after having spun the sample at a different temperature. This forces the  $z$  axis to be oriented, in the  $N_D$  phase for example, as described in figure 3 (a). As we increase the temperature and we enter the biaxial region which 'grows' from the disc phase the  $z$  axis, along which the electric field gradient is higher, is still normal to the magnetic field, as in the  $N_D$  phase.

As the asymmetry parameter increases, with increasing temperature, the  $V_{yy}$  component of the electric field gradient tensor becomes higher and higher till its

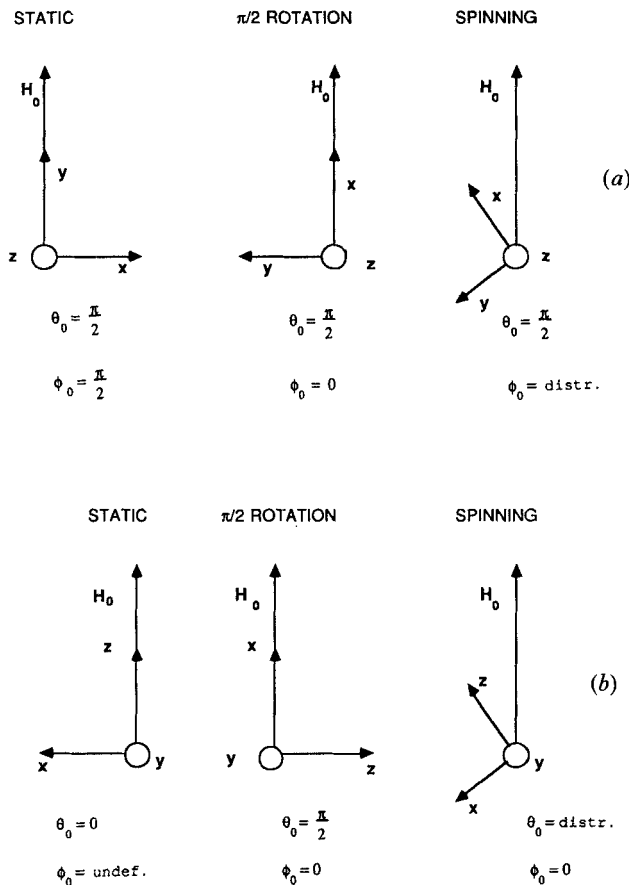


Figure 3. The two possible phase symmetry frames for the  $N_{bx}$  phase in the three different experimental configurations.  $H_0$  is the external magnetic field. Case (a) is valid for  $V_{zz}$  normal to  $H_0$  and case (b) is valid for  $V_{zz}$  along  $H_0$ .



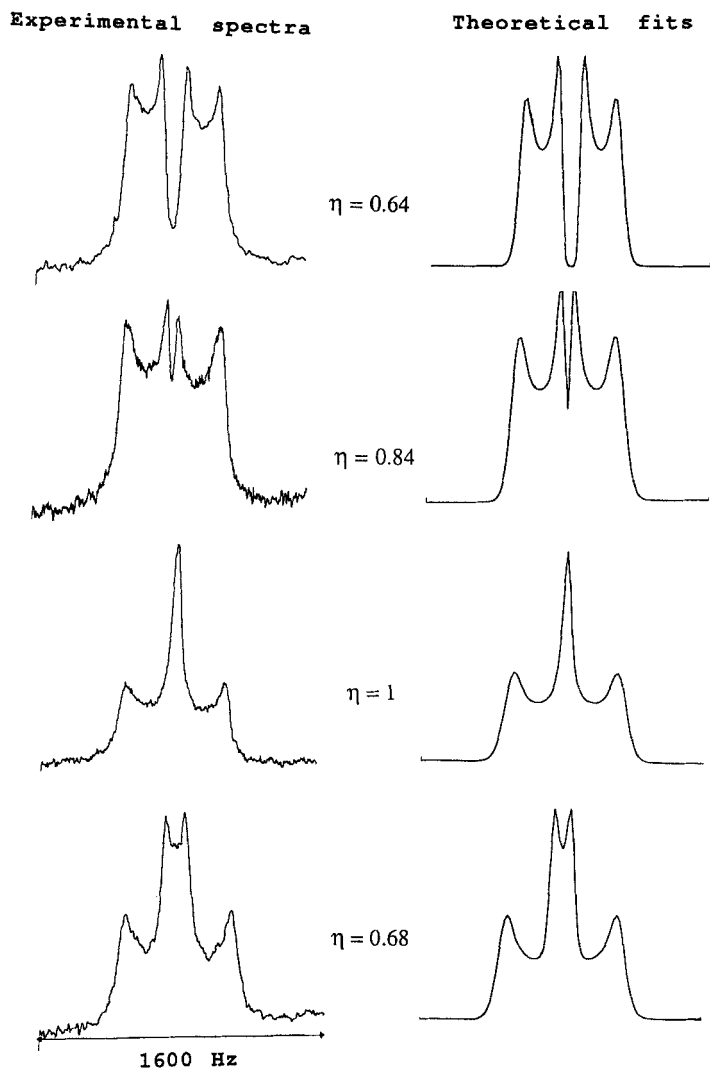


Figure 4. Experimental lineshapes and theoretical fits at different temperatures for the spinning experiments in the biaxial phase for different values of  $\eta$  (sample  $R = 0.1450$ ). Notice how the same value of the biaxiality can result in very different spectra: the spectrum in the first row corresponds to the case shown in figure 3(a) and that in the last row to the case of figure 3(b). The theoretical fits have been obtained by taking into account a line broadening with one component increasing linearly from the centre of the spectrum.

absolute value equals that of  $V_{zz}$  for  $\eta = 1$ . If  $|V_{yy}|$  increases more, then, according to the usual convention for which  $|V_{zz}| > |V_{yy}| > |V_{xx}|$ , which must hold if equation (1) has to be valid, we must change the reference frame to that shown in figure 3(b). This change is underlined by a drastic variation of the lineshape as described in figure 4. Such change of reference frame has no real physical meaning but it allows us to continue to use equation (1) for the deuterium resonance frequency.

If the sample is inserted in the magnet and a spectrum is taken after a  $\pi/2$  rotation without having previously spun the sample, a more complicated spectrum is obtained than those shown in figure 2. Our choice of spinning the samples has then been dictated by the simplification of the spectra, with no loss of information. According to equation (1), for the spinning samples we expect

$$v_{\pm} = \pm \frac{3}{8} \bar{\nu} [-1 + \eta \cos 2\phi_0] \quad (2a)$$

and

$$v_{\pm} = \pm \frac{3}{8} \bar{\nu} [3 \cos^2 \theta_0 - 1 + \eta \sin^2 \theta_0], \quad (2b)$$

with the reported angles distributed over the plane containing  $\mathbf{H}_0$ . Equations (2a) and (2b) correspond to the orientation when the principal axes frame is as in figures 3(a) and (b), respectively. Fitting the observed spectra obtained using equations (2a) and (2b) with such distributions of  $\theta_0$  or  $\phi_0$  is shown in figure 4 together with the experimental lineshapes, for comparison. We point out again that the spinning axis is normal to the plane of the page in figure 3. In this model the shape of the spectra depends on the asymmetry parameter  $\eta$ , which is what we really obtain from the fitting. To obtain the theoretical fits we also introduced a frequency dependent component in the line broadening which increases linearly with the distance from the centre of the spectrum [8]. In such fittings there are then two broadening parameters, one asymmetry parameter,  $\eta$ , and a width parameter,  $\bar{\nu}$ . From equations 2 we notice that the shape of the spectra, in the cases where  $\theta_0$  and  $\phi_0$  are distributed, is determined by  $\eta$  only, since  $\bar{\nu}$  is simply a factor defining the spectral width and the broadening does not substantially affect the lineshape. The factor  $\eta$  is then the main fitting parameter and we were able to obtain values for  $\eta$  within a fitting error of  $\pm 0.02$ . In this way we were able to obtain information on both the value of  $\eta$  at different temperatures and on the orientation of the phase symmetry axes with respect to the external field. Our model is confirmed by the fact that the values of  $\eta$  obtained by fitting the spinning spectra are in excellent agreement with those obtained by considering the modulus of the splittings of the static spectrum,  $\Delta v_s$ , and that of the  $\pi/2$  rotated spectrum,  $\Delta v_{\pi/2}$ :

$$\eta = \frac{\Delta v_s - \Delta v_{\pi/2}}{\Delta v_s + \Delta v_{\pi/2}} \quad (3a)$$

and

$$\eta = \frac{\Delta v_s - 2\Delta v_{\pi/2}}{\Delta v_s}, \quad (3b)$$

which are easily obtained from the splittings of table 2 for both cases shown in figure 3.

In figure 5 we report, for one concentration ( $R = 0.1450$ ), the asymmetry parameter  $\eta$  as derived from static and  $\pi/2$  rotation measurements in the  $N_{bx}$  phase according to equations (3a) and (3b).

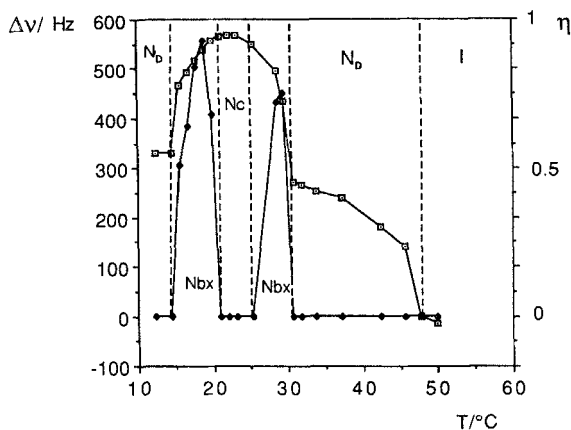


Figure 5. The partially averaged splitting,  $\Delta\nu$  (open dots), and asymmetry parameter,  $\eta$  (full dots), of  $D_2O$  as a function of temperature (sample  $R=0.1450$ ).

A more detailed and precise description of our system requires further data acquisition. In particular, measurements are in progress on samples with deuteriated DaCl and KL, in order to obtain information regarding single amphiphile behaviour. We confirm the high degree of stability of this new system as we did not observe significant changes in the transition temperatures between the different phases over periods of several months.

#### 4. Conclusions

We have studied the phase diagram of the lyotropic system KL/DaCl/ $D_2O$  keeping a fixed molar ratio between the amphiphiles and heavy water and changing the relative molar ratio of the amphiphiles. Three different nematic mesophases have been found, with wide ranges of biaxiality. The biaxial area of the phase diagram has an arc shape similar to that reported in [1] and we found no inversion of the uniaxial mesophases position with temperature. The asymmetry parameter of the averaged electric field gradient tensor on the deuterium of the  $D_2O$  molecules has been measured as a function of temperature and concentration. Measurements on the same system, in which spectra are recorded from deuteriated KL and DaCl, are in progress.

#### References

- [1] YU, L. J., and SAUPE, A., 1980, *J. Am. chem. Soc.*, **102**, 4879; YU, L. J., and SAUPE, A., 1980, *Phys. Rev. Lett.*, **45**, 1000.
- [2] BARTOLINO, R., CHIARANZA, T., MEUTI, M., and COMPAGNONI, R., 1982, *Phys. Rev. A*, **26**, 1116.
- [3] FIGUEIREDO NETO, A. M., GALERNE, Y., LEVELUT, A. M., and LIEBERT, L., 1985, *J. Phys. Lett., Paris*, **46**, L499; FIGUEIREDO NETO, A. M., LIEBERT, L., and GALERNE, Y., 1985, *J. Phys. Chem.*, **89**, 3737.
- [4] CHARVOLIN, J., SAMULSKI, E. T., and LEVELUT, A. M., 1979, *J. Phys. Lett., Paris*, **40**, L587; HENDRIKX, Y., and CHARVOLIN, J., 1981, *J. Phys., Paris*, **42**, 1427.
- [5] OLIVEIRA, E. A., LIEBERT, L., and FIGUEIREDO NETO, A. M., 1989, *Liq. Crystals*, **5**, 1669.
- [6] RADLEY, K., and SAUPE, A., 1978, *Molec. Crystals liq. Crystals*, **44**, 227.
- [7] BAYLE, J. P., BLOSSI, A., GUILLOS, A., and COURTIEU, J., 1987, *Liq. Crystals*, **2**, 665.
- [8] PHOTINOS, D. J., BOS, P. J., DOANE, J. W., and NEUBERT, M. E., 1979, *Phys. Rev. A*, **20**, 2203.
- [9] HARTSHORNE, N. H., and STUART, A., 1964, *Practical Optical Crystallography* (Arnold).
- [10] For a review on the deuterium NMR measurements see: BODEN, N., CORNE, S. A., and JOLLEY, K. W., 1987, *J. Phys. Chem.*, **91**, 4092 and references therein.